Chinese Chemical Letters 33 (2022) 3899–3902

Contents lists available at ScienceDirect

Chinese Chemical Letters

journal homepage: www.elsevier.com/locate/cclet

Two Dawson-type U(VI)-containing selenotungstates with sandwich structure and its high-efficiency catalysis for pyrazoles

Mengyuan Cheng[a,1], Yufeng Liu[b,1], Weixin Du[a], Jingwen Shi[a], Junhua Li[a], Haiying Wang[a], Ke Li[b], Guoping Yang[b,*], Dongdi Zhang[a,*]

[a] Henan Key Laboratory of Polyoxometalate Chemistry, College of Chemistry and Chemical Engineering, Henan University, Kaifeng 475004, China
[b] Jiangxi Province Key Laboratory of Synthetic Chemistry, Jiangxi Key Laboratory for Mass Spectrometry and Instrumentation, East China University of Technology, Nanchang 330013, China

ARTICLE INFO

Article history:
Received 1 November 2021
Revised 16 November 2021
Accepted 17 November 2021
Available online 24 November 2021

Keywords:
Selenotungstates
Uranium
Dawson-type
Condensation reaction
Pyrazoles

ABSTRACT

Two novel uranium-containing selenotungstates $Na_3[H_{19}(UO_2)_2(\mu_2\text{-}O)(Se_2W_{14}O_{52})_2]\cdot 41H_2O$ (**U_2**) and $(NH_4)_{10}[H_4(SeO)_2(UO_2)_2(H_2O)_2(H_2Se_2W_{14}O_{52})(Se_2W_{14}O_{52})]\cdot 66H_2O$ (**Se_2U_2**) based on the $\{Se_2W_{14}O_{52}\}$ unit were successfully prepared and fully characterized. To our knowledge, the uranium is firstly introduced into the selenotungstates. Moreover, it is notable that **U_2** exhibits excellent Lewis acid-base catalytic activities in the condensation cyclization of sulfonyl hydrazides with diketones to synthesize polysubstituted pyrazoles. All the desired products were obtained in moderate to good yields (up to 99%).

© 2022 Published by Elsevier B.V. on behalf of Chinese Chemical Society and Institute of Materia Medica, Chinese Academy of Medical Sciences.

Pyrazoles form an important class of heterocycles and have recently attracted much attention due to a wide range of pharmacological and biological activities [1–3], such as antimicrobial, antibacterial, anti-inflammatory, antifungal, antiproliferative [4,5]. Typical drugs examples containing pyrazole skeletons are celecoxib and rimonabant which have been sale in market [6,7]. Because of the prominent roles, various methods have been reported for the synthesis of pyrazoles [8–10]. Among the reported strategies, the most efficient method is the direct condensation of 1,3-diketones with hydrazines in the presence of acid, such as polystyrenesupported sulfonic acid (PSSA) [11], sulfuric acid [4], $H_2SO_4\cdot SiO_2$ [12], Fe/MWCNTs [13], and so on [14,15]. However, most of the methods suffer from certain drawbacks including long reaction times, unsatisfactory yields, and toxic nonreusable catalyst. Many encouraging advances have been reported, but the development of efficient catalytic systems for pyrazoles is still highly desirable.

Polyoxometalates (POMs) [16,17], large anionic molecular metal-oxygen clusters of the group V and VI elements, have attracted increasing interest because of their strong acid and etching ability in catalysis, magnetism, biomedicine, materials science, and nanotechnology [18–25]. POM ions have ideal multidentate oxygen-donor ligands toward various electrophiles, making them promising candidates for the encapsulation of polynuclear d- and f-block metal-oxo fragments, leading to products with interesting properties [26–30]. In this context, 3d transition metal-containing POM ions represent a large and particularly versatile subclass of POM chemistry [31–36]. Given the same group in the periodic table and the similar behavior in coordination chemistry, we think many POMs long known for 3d or 4f ions should be realized for the actinides. However, only a handful of uranium-containing POMs (UCPOMs) examples are known. Indeed, we are aware of only seven Dawson-type-based UCPOMs since the pioneering work of Pope *et al.* in 1999, in which two $[PW_9O_{34}]^{9-}$ groups sandwich two UO_2^{2+} and two Na^+ cations [37]. In particular, Pope's group has been active in this area, reporting three dimeric and one tetrameric tungstophosphate complexes in 2003, $[U(\alpha_1\text{-}P_2W_{17}O_{61})_2]^{16-}$ (Fig. 1a), $[U(\alpha_1\text{-}P_2W_{17}O_{61})(\alpha_2\text{-}P_2W_{17}O_{61})]^{16-}$ (Fig. 1b), $[U(\alpha_2\text{-}P_2W_{17}O_{61})_2]^{16-}$ (Fig. 1c), and $\{U_{12}(P_2W_{15})_4\}$ (Fig. 1d), in which two isomeric $[P_2W_{17}O_{61}]^{10-}$ units and four $[P_2W_{15}O_{56}]^{12-}$ anions are linked together by one uranium and four trigonal $\{U_3\}$ groups, leading to the first examples of 2:1 type and tetrahedral clusters, respectively [38,39]. In 2008, Kortz *et al.* have reported the first uranium–peroxo derivative of 'P_6W_{36}' ion $\{U_8(P_2W_{12})_3\}$ (Fig. 1e), in which three 'P_2W_{12}' units combine to a gapped ring encircling a central U_8–peroxo moiety [40]. Recently, reaction of the macrocycle $\{P_8W_{48}\}$ precursor with $UO_2(NO_3)_2\cdot 6H_2O$ in formic acid buffer aqueous solution and lithium acetate solution leads to the formation of monodi-

* Corresponding authors.
E-mail addresses: erick@ecut.edu.cn (G. Yang), ddzhang@henu.edu.cn (D. Zhang).
[1] These authors contributed equally to this work.

https://doi.org/10.1016/j.cclet.2021.11.059
1001-8417/© 2022 Published by Elsevier B.V. on behalf of Chinese Chemical Society and Institute of Materia Medica, Chinese Academy of Medical Sciences.

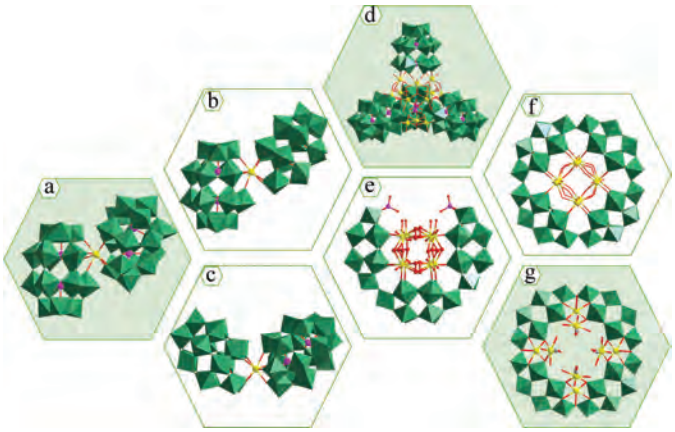

Fig. 1. Summary of the reported Dawson-type of UCPOMs up to now.

mensional chain constructed by $\{U_{7.2}P_8W_{48}\}$ units (Fig. 1f) and a peroxouranium-containing W_{48} wheel $\{[(UO_2)_4(O_2)_4]_2P_8W_{48}\}$ (Fig. 1g), which is isolated by Duval *et al.* and Kortz *et al.* in 2019 and 2020, respectively [41,42].

It should be noted that there are few studies of the potential applications on UCPOMs, and only limited reports on its photochemical properties. To the best of our knowledge, the important application of Lewis acid-base catalytic activity of POMs in organic synthesis has drawn much attention [3,8], but rare catalytic performances of UCPOMs have been reported before. More recently, we have continued our efforts by developing an alternative synthetic strategy by using the template effect of heteroatoms to form new 'open' structures with unsaturated nucleophilic oxygen atoms, which show strong affinity towards electrophilic linkers to construct bigger assemblies. Also, wehave been dedicated to investigate the catalytic activity of POMs for a long time [43–49].

Herein, we present two novel, previously unknown uranium-containing selenotungstates (UCSTs), $Na_3[H_{19}(UO_2)_2(\mu_2\text{-}O)(Se_2W_{14}O_{52})_2]\cdot 41H_2O$ (abbreviated as **U_2**) and $(NH_4)_{10}[H_4(SeO)_2(UO_2)_2(H_2O)_2(H_2Se_2W_{14}O_{52})(Se_2W_{14}O_{52})]\cdot 66H_2O$ (abbreviated as **Se_2U_2**). In contrast with the previously reported complexes mentioned above, two $\{Se_2W_{14}\}$ units are linked together with **U_2** and **Se_2U_2** to give sandwich-dimeric species (Fig. 2). As we know, such a dimeric structure has not yet been observed. The structures have been fully analysed by single-crystal X-ray structure analysis, infrared spectroscopy (IR), thermogravimetric (TG) analysis, and powder X-ray diffraction (PXRD). Moreover, **U_2** as an efficient catalyst to catalyze the condensation cyclization reaction of sulfonyl hydrazides with diketones to synthesize polysubstituted pyrazoles has also been studied.

Compounds **U_2** and **Se_2U_2** were obtained by utilizing a one-pot synthetic strategy employing SeO_3^{2-} as a heterotemplate to generate multivacant selenotungstate (ST) clusters, which can further bind the uranyl UO_2^{2+} cationic group. It is well-known that the self-assembly of POMs is quite sensitive to subtle synthetic parameters, such as pH and counter cations. For **U_2**, $\{\alpha\text{-}Se_2W_{14}\}$ framework was always the preferable product when the pH value was 5.4. Notably, even if **U_2** does not contain any dimethylamine hydrochloride (DMAHC) ligand, its presence during the synthetic process seems crucial since it has not been possible to obtain **U_2** in absence of this reactant. DMAHC was introduced into the reaction system so that it can facilitate enhancement of the solubility of U cations in the Se-O-W system [50]. However, under similar reaction conditions, but with lower pH 4.0 and in the presence of NH_4Cl, the complex **Se_2U_2** is obtained. The two complexes show how it is possible to control the transformation of the clusters (from $\{\alpha\text{-}Se_2W_{14}\}$ to $\{\alpha\text{-}Se_2W_{14}\}$ and $\{\gamma\text{-}Se_2W_{14}\}$) by slightly changing the synthetic conditions.

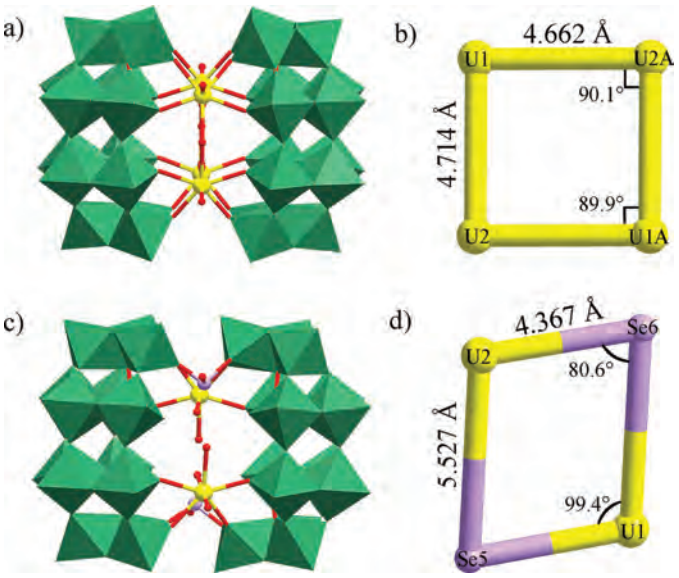

Fig. 2. (a, c) Combined polyhedral/ball-and-stick representations of **U_2** and **Se_2U_2**. (b) Simplified view of the four U^{VI} centers in **U_2**. (d) Simplified view of the central tetra-Se/U^{VI} cluster in **Se_2U_2**. Color code: Se, lavander; W, green; U, yellow; O, red.

Single-crystal X-ray diffraction analysis of the obtained yellow block crystals (Table S1 in Supporting information) reveals that **U_2** and **Se_2U_2** crystallizes in the monoclinic and triclinic system with the space group *C*2/*m* and *P*-1, respectively. **U_2** consists of two identical $\{\alpha\text{-}Se_2W_{14}\}$ units connected by four U^{VI} centers through sixteen terminal oxygen atoms from WO_6 octahedra of each $\{\alpha\text{-}Se_2W_{14}\}$ group (Fig. 2a). Thus, the structure of cluster **U_2** can also be simplistically viewed as two tetravacant $\{\alpha\text{-}Se_2W_{14}\}$ units linked together by four uranium atoms (Fig. S1a in Supporting information). Each of four U atoms is coordinated by four terminal oxygen atoms from two $\{\alpha\text{-}Se_2W_{14}\}$ units with the average bond length of 2.344 Å, one doubly-bridging oxygen atom with the average bond length of 2.509 Å, and two terminal oxo groups, forming a pentagonal bipyramidal coordination geometry (Fig. S1b in Supporting information). The axial U–O bond distances in **U_2** are similar to those in structures previously reported [51], in which the external and the internal bond distances for U1–O28 and U1–O30 are in the range of 1.816–1.836 Å and 1.752–1.818 Å, respectively. The uranyl groups have a small deviation from linearity with angles of 179.6° for O28–U1–O30 and 176.1° for O29–U2–O31, which are within the expected range for the UO_2^{2-} entity. Interestingly, the four U^{VI} centers form a regular rectangle with the edges in the range of 4.662−4.714 Å and the U1−U2A−U1A angle 90.0° (Fig. 2b). It should be noted that crystallographic refinement indicates that occupancy factors of the μ_2-O atoms and the four uranium positions are all 0.5, leading to the formula $[(UO_2)_2(\mu_2\text{-}O)(\alpha\text{-}Se_2W_{14}O_{52})_2]^{22-}$.

The $\{\alpha\text{-}Se_2W_{14}\}$ unit is a tetravacant Dawson fragment which is formed by removing four corner-sharing WO octahedra from the plenary Dawson cluster $\{\alpha\text{-}Se_2W_{18}\}$, and thus it possesses eight unsaturated oxygen atoms, having the potential for further coordination (Fig. 3). Further, the 60° rotation of the two edge-sharing triads of cap-position in $\{\alpha\text{-}Se_2W_{14}\}$ leads to the isomer $\{\gamma\text{-}Se_2W_{14}\}$. Noteworthy, $\{Se_2W_{14}\}$-based structures are rarely observed in POM chemistry. Su and co-workers presented the first examples of $\{Se_2W_{14}\}$-based POM clusters in 2014–2016 [52–54]. Very recently, Zhao *et al.* reported several rare-earth-embedded Dawson ST derivatives [55,56].

Regarding the solid-state structure of **Se_2U_2**, the cluster geometry resembles that of **U_2** but with subtle difference. Firstly, the building units in **U_2** are two identical $\{\alpha\text{-}Se_2W_{14}\}$ fragments, while

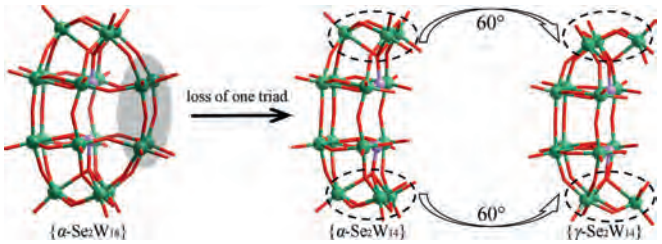

Fig. 3. Ball-and-stick representations of plenary {α-Se_2W_{18}} cluster (left), tetravacant {α-Se_2W_{14}} (middle) and {γ-Se_2W_{14}} (right) segments, highlighting the transformation of {α-Se_2W_{18}} to {α-Se_2W_{14}} and {α-Se_2W_{14}} to {γ-Se_2W_{14}}. Color code: Se, lavander; W, green; O, red.

Table 1
Screening the reaction conditions.[a]

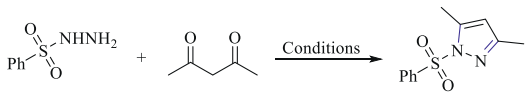

1a **2a** **3a**

Entry	Catalyst (mol%)	Temp. (°C)	*t* (min)	Yield (%)[b]
1	–	r.t.	15	34
2	**U_2** (0.1)	r.t.	15	77
3	**Se_2U_2** (0.1)	r.t.	15	69
4	**U_2** (0.1)	r.t.	30	82
5	**U_2** (0.1)	r.t.	60	85
6	**U_2** (0.1)	60	60	91
7	**U_2** (0.1)	70	60	94
8	**U_2** (0.1)	80	60	97
9	**U_2** (0.2)	80	60	99

[a] Reaction conditions: benzenesulfonyl hydrazide **1a** (1 mmol), acetylacetone **2a** (1 mmol), [Cat.] **U_2** (0.1 mol%).
[b] The yields were determined by GC with biphenyl as the internal standard.

Se_2U_2 comprises two different Dawson fragments. Secondly, two of the four central U^{VI} centers in anion **U_2** have been replaced by two Se^{IV} ions (Fig. S5 in Supporting information). Thirdly, the U^{VI} occupancy factors in **Se_2U_2** are 1 instead of 0.5 in **U_2**. In addition, the central tetra-Se/U^{VI} cluster in **Se_2U_2** can be simplified as a parallelogram with the angles of 80.6° for U1–Se6–U2 and 99.4° for Se6–U1–Se5. Bond-valences sum (BVS) calculations show that the W^{6+} and Se^{4+} centers in **U_2** and **Se_2U_2** are hexacoordinated and tetracoordinated with an octahedral geometry and triangular cone geometry, respectively (Table S2 in Supporting information). Although reports on TM- or RE-substituted STs are burgeoning, the sandwich-type STs are still very limited. Clusters **U_2** and **Se_2U_2** revealed a novel, previously unknown sandwich-type UCST structure. Moreover, **U_2** and **Se_2U_2** are fully characterized by IR, TG and PXRD (Figs. S7-S10 in Supporting information).

Subsequently, in order to explore the catalytic performance of the **U_2** and **Se_2U_2**, they were applied to catalyze the condensation of benzenesulfonohydrazide **1a** and acetylacetone **2a** to evaluate the catalytic activity. The desired product **3a** was obtained with 34% yield at room temperature for 15 min without catalyst (Table 1, entry 1). When the reaction carried out in the presence of **U_2** or **Se_2U_2**, the yields of **3a** increased to 77% and 69%, respectively (entries 2 and 3). These above results indicated that the **U_2** and **Se_2U_2** have catalytic activity for this reaction and the **U_2** perform better. Then, the **U_2** was chosen as catalyst for reaction time screening, the yield of **3a** was improved to 85% with the reaction time increased to 60 min (entries 4 and 5). The results of temperature screening show that increasing the temperature benefited this condensation reaction and the **3a** was obtained in 97% yield at 80 °C (entries 6–8). On further increasing the catalyst loading of **U_2** to 0.2 mol%, the yield of **3a** was obtained in 99% (entry 9).

Table 2
Substrates scope of the cyclization of sulfonyl hydrazides and 1,3-diketones.[a]

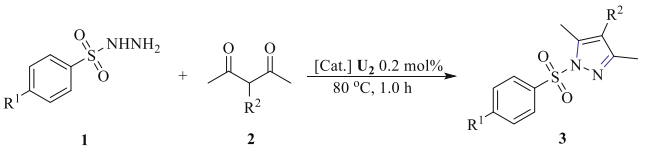

1 **2** **3**

Entry	**1**	**2**	Yield [b]
1	R^1 = H (**1a**)	R^2 = H (**2a**)	**3a**, 99%
2	R^1 = H (**1a**)	R^2 = CH_3 (**2b**)	**3b**, 99%
3	R^1 = H (**1a**)	R^2 = Cl (**2c**)	**3c**, 97%
4	R^1 = H (**1a**)	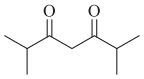 **2d**	**3d**, 99%
5	R^1 = CH_3 (**1b**)	R^2 = H (**2a**)	**3e**, 94%
6	R^1 = CH_3 (**1b**)	R^2 = CH_3 (**2b**)	**3f**, 93%
7	R^1 = CH_3 (**1b**)	R^2 = Cl (**2c**)	**3g**, 95%
8	R^1 = CH_3 (**1b**)	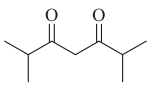 **2d**	**3h** 95%
9	R^1 = Cl (**1c**)	R^2 = H (**2a**)	**3i**, 95%
10	R^1 = Cl (**1c**)	R^2 = CH_3 (**2b**)	**3j**, 95%
11	R^1 = Cl (**1c**)	R^2 = Cl (**2c**)	**3k**, 95%
12	R^1 = Cl (**1c**)	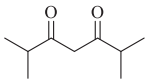 **2d**	**3l**, 98%

[a] Reaction conditions: **1** (1 mmol), **2** (1 mmol), **U_2** (0.2 mol%), 80 °C, 1.0 h.
[b] Isolated yield.

Having the optimized reaction conditions in hand, we next explored the scope of this reaction. All results were summarized in Table 2, acetylacetone **2a**, 3-methylpentane-2,4–dione **2b**, 3-chloropentane-2,4–dione **2c** and 2,6-dimethylheptane-3,5–dione **2d** could react with benzenesulfonohydrazide **1a** smoothly, delivering the desired products **3a**-**3d** in 99%, 99%, 97% and 99% yields, respectively (entries 1–4). Furthermore, the different sulfonyl hydrazines were also tested with the above of four diketone. By using *p*-toluenesulfonhydrazide **1b** as reaction partner, the corresponding products **3e**-**3h** were obtained with 94%, 93%, 95% and 95% yields, respectively (entries 5–8). Further, the 4-chlorobenzenesulfonohydrazide **1c** reacted with acetylacetone **2a, 2b, 2c** and **2d**, giving the desired products **3i**-**3l** in 95%, 95%, 95% and 98% yields, respectively (entries 9–12).

More practically, this reaction could be performed on a gram-scale (5 mmol scale), clearly showing its potential application in organic synthesis (Scheme 1). The model reaction of benzenesulfonohydrazide **1a** and acetylacetone **2a** were investigated under the standard conditions, and the desired product **3a** were obtained in 97% yields, respectively.

Combining the nucleophilic Lewis base surface of POMs with Lewis acid of U cations, the compound **U_2** could function as Lewis acid–base catalysts [3,57] and effectively promote the condensation reaction. As shown in Scheme 2, the U cations in **U_2** act as effective Lewis acid for activation of 1,3-diketones, and the peripheral oxygen atoms of W-O-W species act as Lewis base for activation of sulfonyl hydrazides.

In conclusion, two Dawson-type-{Se_2W_{14}}-based dimeric uranium-containing selenotungstates $Na_3[H_{19}(UO_2)_2(\mu_2\text{-}O)(Se_2W_{14}O_{52})_2]\cdot 41H_2O$ (**U_2**) and $(NH_4)_{10}[H_4(SeO)_2(UO_2)_2(H_2O)_2(H_2Se_2W_{14}O_{52})(Se_2W_{14}O_{52})]\cdot 66H_2O$ (**Se_2U_2**) were successfully prepared and thoroughly characterized. The clusters represent the first examples of Dawson-type UCSTs in POM chemistry. Furthermore,

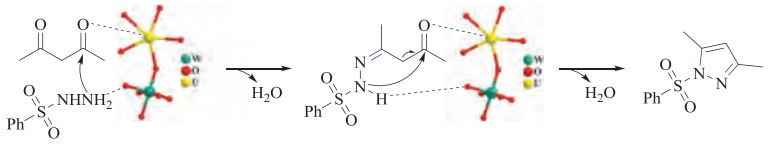

Scheme 2. Proposed mechanism.

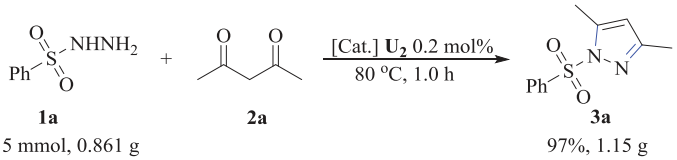

Scheme 1. Gram-scale reactions.

U_2 as an efficient catalyst, the polysubstituted pyrazoles can be synthesized in the condensation cyclization of sulfonyl hydrazides with diketones under moderate conditions to excellent yields. This work may benefit to the development of POMs chemistry, catalytic chemistry and actinides chemistry. Further researches on the synthesis of novel U-containing POMs and their catalytic performance in our group are underway.

Declaration of competing interest

The authors declare no conflict of interest.

Acknowledgements

This work was supported by the National Natural Science Foundation of China (Nos. 22071045, 22001034), Excellent Youth Science Fund Project of Henan Province (No. 202300410042), and the Open Fund of the Jiangxi Province Key Laboratory of Synthetic Chemistry (No. JXSC202008). Dr. D. Zhang thanks for the start-up fund of Henan University.

Supplementary materials

Supplementary data associated with this article can be found, in the online version, at doi:10.1016/j.cclet.2021.11.059.

References

[1] C.W. Wright, J. Addae-Kyereme, A.G. Breen, et al., J. Med. Chem. 44 (2001) 3187–3194.
[2] B. Baruah, P.J. Bhuyan, Tetrahedron 65 (2009) 7099–7104.
[3] G.P. Yang, X.L. Zhang, Y.F. Liu, et al., Inorg. Chem. Front. 8 (2021) 4650–4656.
[4] Z.X. Wang, H.L. Qin, Green Chem. 6 (2004) 90–92.
[5] M. Barceló, E. Raviña, C.F. Masaguer, et al., Bioorg. Med. Chem. 17 (2007) 4873–4877.
[6] Z. Xu, C. Gao, Q.C. Ren, et al., Eur. J. Med. Chem. 139 (2017) 429–440.
[7] R.R. Ranatunge, D.S. Garvey, D.R. Janero, et al., Bioorg. Med. Chem. 12 (2004) 1357–1366.
[8] G. Yang, X. Xie, M. Cheng, et al., Chin. Chem. Lett. 33 (2022) 1483–1487.
[9] M. Kidwai, A. Jain, R. Poddar, J. Organomet. Chem. 696 (2011) 1939–1944.
[10] G. Yang, Y. Liu, X. Lin, et al., Chin. Chem. Lett. 33 (2022) 354–357.
[11] V. Polshettiwar, R.S. Varma, Tetrahedron Lett. 49 (2008) 397–400.
[12] X. Chen, J. She, Z.C. Shang, et al., Synth. Commun. 39 (2009) 947–957.
[13] H. Sharghi, J. Aboonajmi, M. Mozaffari, et al., Appl. Organomet. Chem. 32 (2018) e4124.
[14] G. Cao, G. Zeng, K. Li, et al., Appl. Organomet. Chem. 35 (2021) e6379.
[15] G.P. Yang, X. He, B. Yu, et al., Appl. Organomet. Chem. 32 (2018) e4532.
[16] M.T. Pope, A. Müller, Angew. Chem. Int. Ed. 30 (1991) 34–48.
[17] D.L. Long, R. Tsunashima, L. Cronin, Angew. Chem. Int. Ed. 49 (2010) 1736–1758.
[18] J. Luo, K. Chen, P. Yin, et al., Angew. Chem. Int. Ed. 57 (2018) 4067–4072.
[19] D.Y. Du, J.S. Qin, S.L. Li, et al., Chem. Soc. Rev. 43 (2014) 4615–4632.
[20] J. Zhang, Y. Huang, G. Li, Y. Wei, Coord. Chem. Rev. 378 (2019) 395–414.
[21] Y. Wu, X. Li, Y. Qi, et al., Angew. Chem. Int. Ed. 57 (2018) 8572–8576.
[22] J. Zhang, R. Lai, Y. Wu, et al., Chem. Asian J. 15 (2020) 1574–1579.
[23] M. Zhang, H. Li, J. Zhang, et al., Chin. J. Catal. 42 (2021) 855–871.
[24] D. Zhang, J. Luo, Y. Ma, et al., Inorg. Chem. 59 (2020) 6747–6754.
[25] H. Lin, J.W. Wang, X.W. Guo, et al., J. Mater. Chem. A. 6 (2018) 24479–24485.
[26] X. Chen, Z. Wang, R. Zhang, et al., Chem. Commun. 53 (2017) 10560–10563.
[27] Y.W. Li, L.Y. Guo, H.F. Su, et al., Inorg. Chem. 56 (2017) 2481–2489.
[28] T.P. Hu, Y.Q. Zhao, Z. Jagličić, et al., Inorg. Chem. 54 (2015) 7415–7423.
[29] S.T. Zheng, G.Y. Yang, Chem. Soc. Rev. 41 (2012) 7623–7646.
[30] D. Li, P. Ma, J. Niu, J. Wang, Coord. Chem. Rev. 392 (2019) 49–80.
[31] L. Qiao, M. Song, A. Geng, S. Yao, Chin. Chem. Lett. 30 (2019) 1273–1276.
[32] Z. Zhang, Y. Li, E. Wang, et al., Inorg. Chem. 45 (2006) 4313–4315.
[33] N. Zhang, L. Hong, A. Geng, et al., Chin. Chem. Lett. 29 (2018) 1409–1412.
[34] W. Jiang, X.M. Liu, J. Liu, et al., Chem. Commun. 55 (2019) 9299–9302.
[35] J. Goura, B.S. Bassil, J.K. Bindra, et al., Chem. Eur. J. 26 (2020) 15821–15824.
[36] O. Oms, A. Dolbecq, P. Mialane, Chem. Soc. Rev. 41 (2012) 7497–7536.
[37] K.C. Kim, M.T. Pope, J. Am. Chem. Soc. 121 (1999) 8512–8517.
[38] C. Crăciun, L. David, D. Rusu, et al., J. Radioanal. Nucl. Chem. 247 (2001) 307–310.
[39] A.J. Gaunt, I. May, D. Collison, et al., J. Mol Struct. 656 (2003) 101–106.
[40] S.S. Mal, M.H. Dickman, U. Kortz, Chem. Eur. J. 14 (2008) 9851–9855.
[41] M. Dufaye, S. Duval, G. Stoclet, et al., Inorg. Chem. 58 (2019) 1091–1099.
[42] J. Goura, A. Sundar, B.S. Bassil, et al., Inorg. Chem. 59 (2020) 16789–16794.
[43] G.P. Yang, K. Li, X.L. Lin, et al., Chin. J. Chem. 39 (2021) 3017–3022.
[44] G.P. Yang, X. Wu, B. Yu, et al., ACS Sustain. Chem. Eng. 7 (2019) 3727–3732.
[45] M. Lv, Y. Liu, K. Li, et al., Tetrahedron Lett. 65 (2021) 152757–152760.
[46] J. Jia, Y. Niu, P. Zhang, et al., Inorg. Chem. 56 (2017) 10131–10134.
[47] J. Li, J. Guo, J. Jia, et al., Dalton Trans. 45 (2016) 6726–6731.
[48] H. Wang, L. Hou, C. Li, et al., RSC Adv. 7 (2017) 36416–36420.
[49] W.X. Du, K. Li, D.D. Zhang, et al., Tungsten 4 (2022) 158–167.
[50] H.L. Li, C. Lian, L.J. Chen, et al., Inorg. Chem. 58 (2019) 8442–8450.
[51] H.Y. Wang, X.Y. Zheng, L.S. Long, et al., Inorg. Chem. 60 (2021) 6790–6795.
[52] W.C. Chen, C. Qin, X.L. Wang, et al., Chem. Commun. 50 (2014) 13265–13267.
[53] W.C. Chen, C. Qin, X.L. Wang, et al., Cryst Growth Des. 16 (2016) 2481–2486.
[54] W.C. Chen, C. Qin, Y.G. Li, et al., Chem. Commun. 51 (2015) 2433–2436.
[55] Y. Zhang, B. Zeng, Y. Liu, et al., Eur. J. Inorg. Chem. 35 (2020) 3416–3425.
[56] Y. Zhang, Y. Li, J. Pang, et al., Inorg. Chem. 58 (2019) 7078–7090.
[57] G.P. Yang, S.X. Shang, B. Yu, et al., Inorg. Chem. Front. 5 (2018) 2472–2477.